Diffractive Cross Sections at Low Q^2 from ZEUS

Masahide Inuzuka[a]* on behalf of the ZEUS collaboration

[a]Tokyo Metropolitan University,
Minami-Osawa 1-1, Hachioji-shi, Tokyo 192-0397, Japan

The diffractive cross section $d\sigma^{\rm diff}_{\gamma^* p \to XY}/dM_X$ in the mass range $3.0 < M_X < 12.2\,{\rm GeV}$ and $M_Y < 6.0\,{\rm GeV}$ has been measured at low Q^2, $0.22 < Q^2 < 0.70\,{\rm GeV}^2$, by detecting the scattered electron with the ZEUS Beam Pipe Calorimeter. From the W dependence of the diffractive cross section, the effective intercept of Pomeron trajectory is extracted and compared with the values measured in other Q^2 ranges. It is also compared with the value obtained from the W dependence of the $\gamma^* p$ total cross section in the same Q^2 range.

1. INTRODUCTION

The behaviour of high energy hadron-hadron collisions is described successfully by Regge phenomenology in terms of the Pomeron trajectory, $\alpha_{I\!P}(t) = \alpha_{I\!P}(0) + \alpha'_{I\!P} t$, where t is the momentum transfer squared between the interacting hadrons. The centre-of-mass energy ($\sqrt{s}$) behaviour of the total hadron-hadron cross section is driven by $\alpha_{I\!P}(0)$. The intercept $\alpha_{I\!P}(0)$ was found to be 1.08 by Donnachie and Landshoff [1] using the $\sqrt{s}$ dependence of the hadron-hadron total cross sections; the corresponding result for the slope was $\alpha'_{I\!P} = 0.25\,{\rm GeV}^{-2}$. Such Pomeron trajectory is referred to as 'the soft Pomeron'.

Diffractive scattering at HERA is mediated by Pomeron exchange between the proton and the virtual photon radiated from the initial state electron:

$$\gamma^* + p \to X + Y. \qquad (1)$$

Here $X(Y)$ is the dissociated photon(proton) system whose mass is defined as $M_X(M_Y)$. In the framework of Regge theory the M_X and W dependence of the diffractive cross section is governed by the value of $\alpha_{I\!P}(0)$, where W is the mass of $\gamma^* p$ system.

In photoproduction, where $Q^2 \sim 0$, the $\alpha_{I\!P}(0)$ was obtained by both ZEUS [2] and H1 [3]. Those results as well as the behaviour of the total photoproduction cross section are compatible with that expected from the soft Pomeron. On the other hand, in the large Q^2 region ($Q^2 \gg 1\,{\rm GeV}^2$) where perturbative QCD should be applicable, the value of $\alpha_{I\!P}(0)$ turned out to be significantly higher than that of the soft Pomeron [4,5]. This result might indicate that diffractive processes have different features in the photoproduction and at high Q^2.

In this paper, we concentrate on the investigation of the transition between the photoproduction and DIS. We report the measurement of the Pomeron intercept from the W dependence of diffractive cross sections in the region $0.22 < Q^2 < 0.70\,{\rm GeV}^2$ using the ZEUS Beam Pipe Calorimeter.

2. ANALYSIS

The ZEUS Beam Pipe Calorimeter (BPC) is a tungsten-scintillator sampling calorimeter, which sits close to the beam pipe 3m downstream of the interaction point in the electron beam direction [6]. The low Q^2 events were tagged by requiring the identification of the scattered electrons in the BPC. The kinematic variables Q^2 and W are reconstructed from the measured energy and scattered angle of the final state electrons in the BPC. In this analysis, events with $0.22 < Q^2 < 0.70\,{\rm GeV}^2$ and $90 < W < 200\,{\rm GeV}$ were selected.

The invariant mass distribution of the hadronic final state M_H is used in order to separate the diffractive contribution from the non-diffractive

*Supported by Research Fellowships of the Japan Society for the Promotion of Science for Young Scientists.

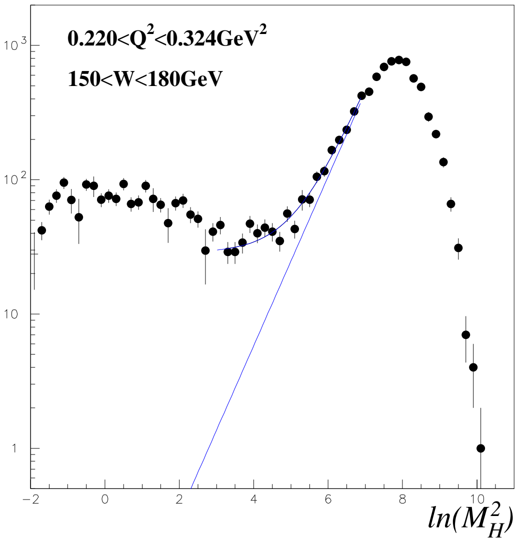

Figure 1. The $\ln M_H^2$ distribution at low Q^2.

contribution [4]. The mass M_H is reconstructed from the energy deposits in the uranium calorimeter and track momenta measured in the central tracking chambers for the charged particles. Fig.1 shows the distribution of the logarithm of M_H^2. The distribution exhibits two distinctive components; one is from diffractive events at low mass and the other is from non-diffractive events at high mass.

In the case of diffractive processes, there is a rapidity gap between the hadronic systems X and Y. Since hadrons from the dissociated proton are well collimated along the beam direction in the laboratory frame, the M_H represents well the mass of dissociated photon M_X. On the other hand, the probability of containing a large rapidity gap is small for non-diffractive events. Assuming uniform, random and uncorrelated particle emission along the rapidity axis, the $\ln M_H^2$ distribution is expected to show an exponential fall-off behaviour at high mass towards smaller values [4].

We therefore fitted the distribution to the form

$$\frac{dN}{d\ln M_H^2} = D + c\exp(b\ln M_H^2). \qquad (2)$$

The resulting curve and exponential slope are drawn in Fig.1. Using this result, the non-diffractive contribution was subtracted statistically to obtain the diffractive contribution.

3. RESULTS

The diffractive cross section $d\sigma^{\mathrm{diff}}_{\gamma^* p}/dM_X$ was measured from the number of diffractive events found as described in the previous section. Fig.2 shows the cross section for different Q^2 and M_X bins as a function of W. The inner error bars show the statistical errors and the full bars are the statistical and systematic errors added in quadrature.

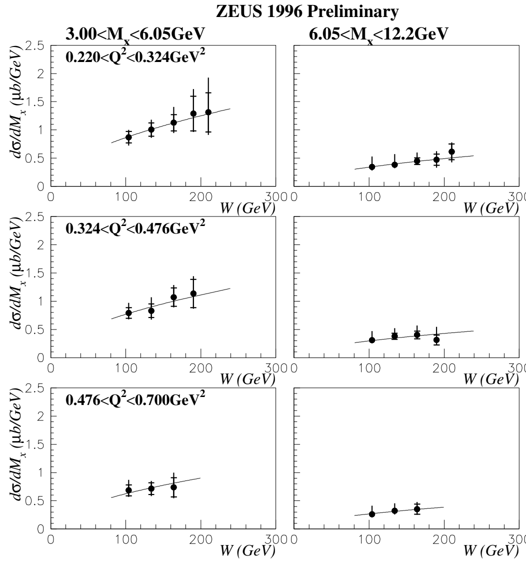

Figure 2. Diffractive cross sections for different Q^2 and M_X ranges as a function of W.

According to the Regge formalism, the diffractive cross section can be expressed as

$$\frac{d^2\sigma^{\mathrm{diff}}_{\gamma^* p}}{dt dM_X} \propto (W^2)^{2\alpha_{I\!P}(0)-2} \cdot e^{t(b+2\alpha'_{I\!P} ln\frac{W^2}{M_X^2+Q^2})}, \quad (3)$$

where t is the four momentum transfer squared at the proton vertex. Since the t distribution was not measured in this analysis, the measured cross section is integrated over t. The W dependence of the diffractive cross section can be written with the effective Pomeron intercept $\bar{\alpha}_{I\!P}$ as

$$\frac{d\sigma^{\text{diff}}_{\gamma * p}}{dM_X} \propto (W^2)^{2\bar{\alpha}_{I\!P}-2}. \tag{4}$$

The value of $\bar{\alpha}_{I\!P}$ is related to $\alpha_{I\!P}(0)$ by

$$\bar{\alpha}_{I\!P} = \alpha_{I\!P}(0) - \alpha'_{I\!P} \cdot |\bar{t}|, \tag{5}$$

where $|\bar{t}|$ is the mean value of $|t|$.

Under the assumption that $\bar{\alpha}_{I\!P}$ does not vary with Q^2 and M_X, the cross section $d\sigma^{\text{diff}}_{\gamma^* p}/dM_X$ can be fitted to the form

$$\frac{d\sigma^{\text{diff}}_{\gamma^* p}}{dM_X} = A \cdot W^{2(2\bar{\alpha}_{I\!P}-2)} \tag{6}$$

for each Q^2 and M_X bin. The curves in Fig.2 are the result of the fit. The effective Pomeron intercept is found to be

$$\bar{\alpha}_{I\!P} = 1.133 \pm 0.026(stat)^{+0.043}_{-0.062}(syst). \tag{7}$$

Assuming $\alpha'_{I\!P} = 0.25\text{GeV}^{-2}$ and $|\bar{t}| = 1/7.5\text{GeV}^2$, $\alpha_{I\!P}(0)$ is calculated from relation (5). In Fig.3, the value is shown as a star, and is compared with the photoproduction and DIS results [2–5]. For a comparison, the curve in the figure shows the $\alpha_{I\!P}(0)$ obtained from the ALLM97 parametrization [7]. Our result is consistent with the result obtained from the W dependence of the $\gamma^* p$ total cross section in the same Q^2 range, shown as a closed circle in Fig.3.

4. SUMMARY

The cross section of the diffractive process (1) in the mass range $3.0 < M_X < 12.2\,\text{GeV}$ and $M_Y < 6.0\,\text{GeV}$ in the low Q^2 region, $0.22 < Q^2 < 0.70\,\text{GeV}^2$, has been measured with the ZEUS detector.

Taking advantage of the shape difference of the $\ln M_H^2$ distributions, the diffractive contribution was separated from the non-diffractive contribution to obtain the diffractive cross section $d\sigma^{\text{diff}}_{\gamma^* p}/dM_X$.

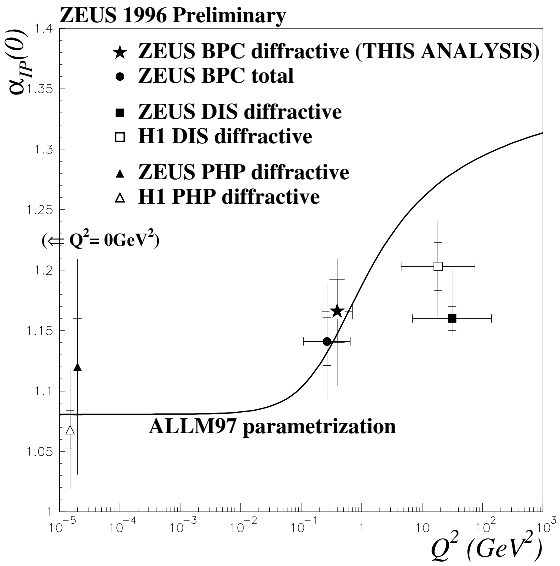

Figure 3. The experimental results of $\alpha_{I\!P}(0)$ in different Q^2 regions.

The effective intercept of Pomeron trajectory was measured to be

$$\bar{\alpha}_{I\!P} = 1.133 \pm 0.026(stat)^{+0.043}_{-0.062}(syst)$$

from the W dependence of $d\sigma^{\text{diff}}_{\gamma^* p}/dM_X$. The obtained value is consistent with the result from the $\gamma{*}p$ total cross section in the same Q^2 range.

REFERENCES

1. A. Donnachie and P.V. Landshoff. Phys. Lett. **B296** (1992) 227.
2. ZEUS Collab. J. Breitweg et al. Z.Phys. **C75** (1997) 421.
3. H1 Collab. C. Adloff et al. Z.Phys. **C74** (1997) 221.
4. ZEUS Collab. J. Breitweg et al. Eur. Phys. J. **C6** (1999) 43.
5. H1 Collab. C. Adloff et al. Z.Phys. **C76** (1997) 613.
6. ZEUS Collab. M. Derrick et al. Z.Phys. **C69** (1996) 607.
7. H. Abramowicz and A. Levy. DESY 97-251.